Published in final edited form as:
Biochim Biophys Acta. 2009 October ; 1793(10): 1604–1613. doi:10.1016/j.bbamcr.2009.07.001.

Transcriptional coupling of synaptic transmission and energy metabolism: Role of nuclear respiratory factor 1 in co-regulating neuronal nitric oxide synthase and cytochrome c oxidase genes in neurons

Shilpa S. Dhar, **Huan Ling Liang**, and **Margaret T. T. Wong-Riley***
Department of Cell Biology, Neurobiology, and Anatomy, Medical College of Wisconsin, Milwaukee, Wisconsin 53226 USA

SUMMARY

Neuronal activity is highly dependent on energy metabolism; yet, the two processes have traditionally been regarded as independently regulated at the transcriptional level. Recently, we found that the same transcription factor, nuclear respiratory factor 1 (NRF-1) co-regulates an important energy-generating enzyme, cytochrome c oxidase, as well as critical subunits of glutamatergic receptors. The present study tests our hypothesis that the co-regulation extends to the next level of glutamatergic synapses, namely, neuronal nitric oxide synthase, which generates nitric oxide as a downstream signaling molecule. Using *in silico* analysis, electrophoretic mobility shift assay, chromatin immunoprecipitation, promoter mutations, and NRF-1 silencing, we documented that NRF-1 functionally bound to *Nos1*, but not *Nos2* (inducible) and *Nos3* (endothelial) gene promoters. Both *COX* and *Nos1* transcripts were up-regulated by depolarizing KCl treatment and down-regulated by TTX-mediated impulse blockade in neurons. However, NRF-1 silencing blocked the up-regulation of both *Nos1* and *COX* induced by KCl depolarization, and over-expression of NRF-1 rescued both *Nos1* and *COX* transcripts downregulated by TTX. These findings are consistent with our hypothesis that synaptic neuronal transmission and energy metabolism are tightly coupled at the molecular level.

Keywords

gene regulation; EMSA; NRF-1 over-expression; rat primary neurons; transcription factor; TTX

INTRODUCTION

Nitric oxide (NO) is a short-lived radical that acts via a second messenger (cGMP) with many diverse actions in the nervous, vascular, and immune systems [1–2]. Nitric oxide synthase (NOS) is responsible for NO production by catalyzing the conversion of L-arginine to L-citrulline in an NADPH and calcium/calmodulin-dependent reaction [3]. NOS constitutes a

***Corresponding author:** Margaret T. T. Wong-Riley, Ph.D., Department of Cell Biology, Neurobiology, and Anatomy, Medical College of Wisconsin, 8701 Watertown Plank Road, Milwaukee, WI 53226, Telephone: 414-456-8467, Fax: 414-456-6517, Email: mwr@mcw.edu.

family of three distinct isoforms: neuronal (NOS1 or nNOS), inducible (NOS2 or iNOS), and endothelial (NOS3 or eNOS) [3–5]. In many brain areas, NOS1 is activated by the influx of Ca^{2+} via glutamatergic NMDA receptors, inducing the binding of calmodulin and the generation of NO, which functions as a signaling molecule through the cGMP pathway [6–7]. Excitatory glutamatergic transmission is highly energy-dependent, as membrane repolarization after depolarization requires ATP-dependent Na^+/K^+ ATPase to actively pump cations against their concentration and electrical gradients, whereas repolarization after hyperpolarization is mainly passive [8]. Thus, neuronal activity, especially of the excitatory type, and energy metabolism are tightly coupled processes [8]. Regions with a higher concentration of glutamatergic synapses than GABAergic synapses are also rich in cytochrome c oxidase (COX) [9], a critical energy-generating enzyme that catalyzes the final step of oxidative metabolism [8,10]. When excitatory transmission is suppressed, such as with TTX-induced impulse blockade, the level of COX as well as of NMDA receptors and NOS1 are reduced [11–12].

Recently, we found that the coupling between glutamatergic synapses and oxidative metabolism exists at the transcriptional level. Essential NMDA receptor subunit 1 as well as subunit 2b and all subunits of COX are regulated by the same transcription factor, nuclear respiratory factor 1 (NRF-1) [13–14], a transcription factor known to be critical for mitochondrial biogenesis [15–16]. As a putative NRF-1 binding site has been reported for human *Nos1* gene but not functionally characterized [17], we sought to determine if NRF-1 indeed directly regulates the expression of *Nos1* in murine neurons. Using multiple approaches, we document in the present study that NRF-1 functionally regulates the expression of *Nos1* in rodent neurons, but via a site different from the one reported by Hall et al. in humans (1994).

MATERIALS AND METHODS

All experiments were carried out in accordance with the US National Institutes of Health Guide for the care and use of laboratory animals and the Medical College of Wisconsin regulations. All efforts were made to minimize the number of animals and their suffering.

Cell culture

Murine neuroblastoma (N2a) cells (ATCC, CCL-131) were grown in Dulbecco's modified Eagle's medium supplemented with 10% fetal bovine serum, 50 units/ml penicillin, and 100 μg/ml streptomycin (Invitrogen, Carlsbad, CA) at 37°C in a humidified atmosphere with 5% CO_2.

Sprague Dawley rats (Harlan, Indianapolis, IN) at 1 day of age were used for primary cultures. Rat primary visual cortical neurons were cultured as described previously [18]. Briefly, 1-day-old neonatal rat pups were sacrificed by decapitation. Brains were removed from the skull and the meninges were removed. Visual cortical tissue was dissected, trypsinized, and triturated to release individual neurons. Neurons were plated in 35 mm poly-L-lysine-coated dishes at a density of 50,000 cells/dish. Cells were maintained in Neurobasal-A media supplemented with B27 (Invitrogen). Ara-C (Sigma, St. Louis, MO) was added to the media to suppress the proliferation of glial cells.

Murine NOS isoform gene promoters analysed by *in silico* analysis

DNA sequences surrounding the transcription start points (TSPs) of NOS isoform genes (*Nos1, 2,* and *3*) were derived from the mouse genome database in GenBank™ using Genomatix Gene2promoter software as well as NCBI GenBank. These promoter sequences encompassed 1 kb upstream and up to 1kb downstream of the TSP of each gene analyzed. Computer-assisted search for putative NRF-1 core binding sequences "GCGCA(T/C)GC" or "GCGCA(G/C)GC"

was conducted on each promoter sequence. Alignment of human, mouse, and rat promoter sequences were done as previously described, using the Genome VISTA genome alignment tool [13,18]. Mouse *Nos1, 2*, and *3* promoter sequences were compared with rat and human genomic sequences using a 5-bp calculation window. Regions of high homology and/or contain putative NRF-1 binding sites were compared for the conservation of NRF-1 binding.

In vitro interactions via electrophoretic mobility shift (EMSA) and supershift assays

EMSAs to assay NRF-1 interactions with putative binding elements on NOS isoform genes were carried out with methods as previously described [13]. Briefly, oligonucleotide probes with putative NRF-1 binding site on each promoter (*Nos1–3*) (Table 2A, based on *in silico* analysis) were synthesized. These oligonucleotides were annealed, and labeled by a Klenow fragment fill-in reaction with [α-^{32}P] dATP (50 μCi/200 ng). Each labeled probe was incubated with 2 μg of calf thymus DNA and 5 μg of HeLa nuclear extract (Promega, Madison, WI) and processed for EMSA. Supershift assays were also performed and, in each reaction, 1–1.5 μg of NRF-1-specific antibodies (polyclonal goat antibodies, gift of Dr. Richard Scarpulla, Northwestern University, Chicago, IL) were added to the probe/nuclear extract mixture and incubated for 20 min at room temperature. For competition, 100-fold excess of unlabeled oligonucleotides were incubated with nuclear extract before adding labeled oligonucleotides. Shift reactions were loaded onto 4% polyacrylamide gel and ran at 200 V for 2.5 h in 0.25X TBE buffer. Results were visualized by autoradiography. Rat cytochrome *c* with NRF-1 binding site at position −172/−147 was designed as previously described [15] and used as a positive control. NRF-1 mutants with mutated sequences as shown in Table 2A were used as negative controls.

In vivo interactions using chromatin immunoprecipitation (ChIP) assays

ChIP assays were performed similar to those described previously [13]. Briefly, ~750,000 N2a cells were used for each immunoprecipitation and were fixed with 1% formaldehyde for 10 min at room temperature. ChIP assay kit (Upstate, Charlottesville, VA) was used with minor modifications. Following formaldehyde fixation, cells were resuspended in a swelling buffer (5 mM PIPES, pH 8.0, 85 mM KCl, and 1% Nonidet P-40, and protease inhibitors added right before use) and homogenized 10 times in small pestle Dounce tissue homogenizer (7 ml). Nuclei were then isolated by centrifugation before being subjected to sonication. The sonicated lysate was immunoprecipitated with either 0.2 μg of NRF-1 polyclonal rabbit antibodies (gift of Dr. Scarpulla) or 2 μg of anti-nerve growth factor receptor (NGFR) p75 polyclonal goat antibodies (C20, sc-6188, from Santa Cruz Biotechnology, Santa Cruz, CA). Semi-quantitative PCR was performed using 1/20th of precipitated chromatin. Primers targeting promoter sequences near TSP of *Nos1–3* genes were designed (Table 2B) as previously described [18]. The promoter of transcription factor B2 of mitochondria (TFB2M), previously found to be activated by NRF1 [19–20], was used as a positive control, whereas exon 5 of β-actin gene was used as a negative control (Table 2B). PCR reactions were carried out with the EX Taq hot-start polymerase (Takara Mirus Bio, Madison, WI) with the following cycling parameters: 30-s denaturation at 94°C, 30-s annealing at 59.5°C, and 20-s extension at 72°C (32–36 cycles per reaction). All reactions were hot-started by heating to 94°C for 120 s. Use of hot-start polymerase and PCR additives significantly improved the quality and reproducibility of ChIP. PCR products were visualized on 2% agarose gels stained with ethidium bromide.

Promoter mutagenesis study

Luciferase reporter constructs of *Nos1* promoters were made by PCR cloning the proximal promoter sequences using genomic DNA prepared from mouse N2a cells as template, digested with *HindIII* and *KpnI* restriction enzymes, and ligated directionally into pGL3 basic vector (Promega).

Sequences of primers used for PCR cloning and mutagenesis are provided in Table 2C. Subunit *COX6b1* clone was used as previously described [13]. Site-directed mutagenesis of putative NRF-1 binding site on each promoter was generated using QuikChange site-directed mutagenesis kit (Stratagene, La Jolla, CA). Both constructs were verified by sequencing.

Each promoter construct (*Nos1* and *COX6b1*) was transfected into N2a cells in a 24-well plate using Lipofectamine 2000. Each well received 0.6 μg of promoter construct and 0.03 μg of pCMVβgal, which constitutively expressed β-galactosidase. After 48 h of transfection, cell lysates were harvested and measured for luciferase activity as described previously [13].

To further investigate the effect of KCl stimulation after mutating the NRF-1 binding site, transfected neurons were stimulated with KCl at a final concentration of 20 mM in the culture media for 5 h as previously described [21]. Cell lysates were then harvested and measured for luciferase activity as described previously [13].

NRF-1 shRNA plasmid construction

NRF-1 silencing was carried out using small hairpin RNAs (shRNA) against murine NRF-1 (GenBankTM accession no. for NRF-1: NM_010938) cloned into pLVTHM vector with H1 promoter and green fluorescent protein reporter (gift of Dr. P. Aebischer, Swiss Federal Institute of Technology). Four shRNA sequences were selected: 5'-GAAAGCTGCAAGCCTATCT-3'; 5'-GCCACAGGAGGTTAATTCA-3'; 5'-GCATTACGGACCATAGTTA-3'; and 5'-AGAGCATGATCCTGGAAGA-3', with a linker sequence (5'-TTCAAGAGA- 3') and complementary sequence for each to form the NRF-1-shRNA cassette. Multiple shRNA sequences enhance the efficiency of gene silencing [22–23]. The pLL3.7/U6 promoter vector with puromycin resistance (Addgene, Cambridge, MA) vector was used concurrently for puromycin selection. The empty vector pLVTHM or scrambled shRNA in pLVTHM served as negative controls. The basic gene cloning method was followed as described previously [13,20]. N2a cells or primary neurons were plated in 35-mm dishes at a density of 5 to 8 × 10^6 cells/dish. They were co-transfected 3 days post-plating with NRF-1 shRNA expression vectors (four sequences at equal amounts; 4 μg total for N2a cells and 1 μg total for primary neurons) and the pLL3.7/U6 vector for puromycin resistance (1.5 μg for N2a cells and 1 μg for primary neurons) via Lipofectamine 2000. Empty vectors or scrambled shRNA vectors alone were used at the same concentrations as vectors with shRNA against NRF-1. Puromycin at a final concentration of 0.5 μg/ml was added to the culture medium on the second day after transfection to select for purely transfected cells. Green fluorescence was observed to monitor transfection efficiency. Transfection efficiency for N2a cells ranged from 40% to 75%, while that for primary cortical neurons was from 40% to 60%. However, puromycin selection effectively yielded 100% of transfected cells. Cells were harvested after 48 h of silencing and lysed for either protein or total RNA preparation.

To determine the effect of KCl stimulation, N2a cells transfected with shRNA against NRF-1 were exposed to KCl at a final concentration of 20 mM in the culture media for 5 h as previously described [21]. Cells were then harvested for RNA isolation.

RNA Isolation and cDNA Synthesis

Total RNA was isolated by RNeasy kits (Qiagen, Valencia, CA) according to the manufacturer's instructions. Three micrograms of total RNA was treated with DNase I and purified by phenolchloroform. cDNA was synthesized using random hexamer primers and SuperScript^{TM} II RNase H-Reverse Transcriptase (Invitrogen) according to the manufacturer's instructions.

Real-time Quantitative PCR

Real-time quantitative PCRs were carried out in a Cepheid Smart Cycler Detection system (Cepheid, Sunnyvale, CA). SyBr Green (BioWhittaker Molecular Application) and EX Taq realtime quantitative PCR hotstart polymerase were used following the manufacturer's protocols and as described previously [13]. Primer sequences are shown in Table 3. PCR runs: hot start 2 min at 95°C, denaturation 10 s at 95°C, annealing 15 s according to the T_m of each primer, and extension 10 s at 72°C for 15–30 cycles. Melt curve analyses verified the formation of single desired PCR product. Mouse β-actin for N2a cells and rat 18s for primary neurons was used as the internal control and the $2\text{-}\Delta\Delta\boldsymbol{C}_T$ method [24] was used for the relative amount of transcripts. Subunits *COX2* (mitochondrial-encoded) and *COX6c* (nuclear-encoded) were used as previously described [13].

Western Blot Assays

Control and NRF-1 shRNA samples were lysed with lysis buffer (0.5% Triton-X-100 and 5 mM ethylenediamine-tetraacetic acid (EDTA) in PBS with 1× complete protease inhibitor) and centrifuged. The concentration of the supernatant was measured with the Bio-Rad protein Assay Kit II (Bio-Rad, Hercules, CA, USA). A total of 50 μg proteins were loaded onto each lane of 10% SDS-PAGE gels and electrophoretically transferred onto polyvinylidene difluoride membranes (Bio-Rad, Hercules, CA). Subsequent to blocking, blots were incubated in primary antibodies (polyclonal antibodies against NRF-1 (1:500; gift of Dr. Scarpulla,), NOS1 (monoclonal antibodies, 1:200; N2280, Sigma), or NOS2 (1:200; sc-7271, C11 from Santa Cruz Biotechnology). Monoclonal antibodies against β-actin (A5316, Sigma) at 1:3,000 dilutions were used as loading controls. Blots were then incubated in secondary antibodies (goat-anti-rabbit, goat-anti-mouse, or rabbit-anti-goat; Chemicon), reacted with ECL, and exposed to autoradiographic film (Santa Cruz Biotechnology). Quantitative analyses of relative changes were done with Personal Molecular Imager, with Quantity one 1-D analysis software (Bio-Rad).

NRF-1 overexpression and TTX treatment

pSG5NRF-1 expression plasmid, a generous gift from Dr. Richard Scarpulla [25], was used for NRF-1 over-expression. N2a cells and primary neurons were each plated in 35 mm dish at a density of 2 to 5×10^5 cells/dish. N2a cells were co-transfected 3 days post-plating with either 2.5 μg of the pSG5NRF-1 plasmid or an empty vector plus 0.5 μg of pLL3.7 Puro vector, using Lipofectamine 2000 (Invitrogen) at a 1:3 ratio. Procedures were identical for the transfection of primary neurons, except that 2 μg pSG5NRF-1 plasmids were used. Puromycin at a final concentration of 0.5 μg/ml was added on the second day after transfection to select for purely transfected cells. After one day of over-expression, TTX at a final concentration of 0.4 μM was added to the culture media for 3 days. N2a cells and primary neurons were harvested on the 4^{th} day for RNA isolation.

Statistical Analysis

Significance among group means was determined by analysis of variance (ANOVA). Significance between two groups was analyzed by Student's *t* test. *P*-values of 0.05 or less were considered significant.

RESULTS

Promoter analysis of NOS genes by means of *in silico* analysis

The proximal promoters of murine *Nos1*, *2*, and *3* genes were analyzed using *in silico* analysis with DNA sequence 1 kb 5' upstream and 1 kb beyond 3' of transcription start point (TSP). The sequence (GCGCGTGTGCGC) reported but not functionally characterized by Hall *et*

al. (1994) to be the putative NRF-1 binding site in the human *Nos1* gene has no homology in either the mouse or rat *Nos1* gene; thus we were not able to use it for the present study. Moreover, it lacks a GCA core found by us to be invariant for NRF-1 binding in the genes that we have analyzed thus far in neurons [13,14,26] and is present in the traditional NRF-1 sequence [15]. In searching further for putative NRF-1 binding site even 2 kb upstream and downstream of TSP, we could find only a single site with GC-rich sequences flanking a GCA core (GCGAGCAGAGCGGCGC) in exon 1 coding region of murine *Nos1* gene designated by Genomatix as a promoter region (Gene ID 18125, Genomatix GXP_435815, NCBI NT_078458, and ENSMUST00000102557). It bore a high (85–95%) homology with both the rat and human *Nos1* genes (Table 1). This region was also rich in putative binding sites for other transcription factors, such as NRF-2, Sp1, and CREB (unpublished observations).

At least twelve alternative exon 1 have been identified in the human *Nos1* gene, and transcription is partially controlled by exon 1- specific promoter sequences [27,28]. In mice, five alternatively spliced variants and one unspliced form encoding five different isoforms of protein have been reported, and our NRF-1 core binding sequence matched two of the splice variants, aSep07Nos1 and bSep07Nos1, found also in vivo [29]. This diversity of alternative promoters and *Nos1* transcripts probably helps to control the diversity of *Nos1* expression in many different organs [27]. Transcriptional regulatory element has been found in the coding sequence in a number of genes [30–32].

Nos2 and *Nos3* promoters, on the other hand, lack both typical and atypical NRF-1 binding sites. Thus, we selected from a region close to the TSP with some GC and a GCA sequence for each of the genes as probes for electrophoretic mobility shift assays.

In vitro NRF-1 interactions with NOS promoters

Electrophoretic mobility shift assays (EMSAs) for NRF-1 interactions were carried out in vitro using ^{32}P-labeled oligonucleotide probes to determine the specificity of NRF-1 binding to murine NOS promoters (*Nos1*, *Nos2* and *Nos3*) (Fig. 1). Rat cytochrome c promoter with known NRF-1 site at positions −172/−147 [15] served as a positive control and it formed specific DNA/NRF-1 shift and supershift complexes (Fig. 1, lanes 1 and 3, respectively). When an excess of unlabelled probe was added as a competitor, no shift band was formed (Fig. 1, lane 2). *Nos1* promoter formed a specific DNA-protein shift complex when incubated with HeLa nuclear extract (Fig. 1, lane 5) and a DNA-protein-antibody supershift complex with the addition of NRF-1 antibodies (Fig. 1, lane 8). Competition with excess unlabelled probe eliminated the shift complex (Fig. 1, lanes 6 and l0, respectively), whereas an excess of unlabeled mutant NRF-1 probes was not able to compete (Fig. 1, lane 7). To rule out any non-specific antibody and oligonucleotide interaction, labeled probes were incubated with NRF-1 antibody without HeLa nuclear extract, and no shift bands were observed (Fig. 1, lane 4). *Nos1* probe with mutated NRF-1 site showed neither shift nor supershift complex (Fig. 1, lanes 9 and 11, respectively). *Nos2* and *Nos3* lacked both typical and atypical NRF-1 binding sites and did not yield any shift bands (Fig. 1, lanes 12–13), verifying our previous report that the presence of a GCA core flanked by GC-rich sequences are essential for NRF-1 binding in neurons [13–14,26].

In vivo interaction of NRF-1 with *NOS* isoform genes

To verify NRF-1 interactions with *NOS* isoform genes in vivo, chromatin immunoprecipitation assays (ChIP) were performed. PCRs that targeted NOS isoform promoters surrounding putative NRF-1 binding sites were carried out in parallel on chromatin immunoprecipitated from N2a cells. A 0.5 and 0.1 % dilution of input chromatin (i.e. prior to immunoprecipitation) was used as a standard to indicate the efficiency of the PCRs. The proximal promoters of *Nos1–3* isoforms in the presence of nuclear extract were subjected to chromatin immunoprecipitation

with NRF-1 antibodies. *Nos1* and *TFB2M* each produced a band from DNA immunoprecipitated with anti-NRF-1 antibodies at a position identical to that of the genomic DNA control (input) (Fig. 2). On the other hand, *Nos2*, *Nos3* and β-actin yielded no bands (Fig. 2). In all cases, immunoprecipitation with NGFR antibodies, an additional negative control, did not yield any PCR product, confirming the specificity of the ChIP reaction.

Mutational analysis for *Nos1* and *COX6b1* promoters

Based on EMSA probes (Table 2A) that formed NRF-1 specific complexes (Fig. 1), site-directed mutagenesis of these same putative NRF-1 binding sites on *Nos1* and known murine *COX6b1* [13] promoters were constructed (Table 2C), generated in luciferase reporter plasmids, and analyzed by gene transfection. As shown in Figure 3, mutation of NRF-1 binding sites led to ~ 61 – 66% reduction in promoter activity of *Nos1* and *COX6b1* genes, respectively ($P < 0.05 – 0.001$). *COX6b1* subunit promoter served as a positive control and confirmed our previous report [13].

Knockdown of NRF-1 by RNA interference

To determine the effect of NRF-1 knockdown on the expression of NOS, plasmid vectors expressing small hairpin RNA (shRNA) against target sequences of NRF-1 mRNA were used. These vectors were previously found to suppress NRF-1 expression in N2a cells [13]. Transfection of neurons with shRNA vectors resulted in ~ 70 – 85% decrease in levels of NRF-1 and NOS1, but not of NOS2, proteins as measured by western blots ($P < 0.05 – 0.01$) (Fig. 4A). cDNAs from N2a cells (Fig. 4B) and primary neurons (Fig. 4C) transfected with NRF-1 shRNA vectors, scrambled shRNA vectors, or empty vectors were analyzed with quantitative real-time PCRs. As shown in Figures 4B and 4C, relative mRNA levels of *NRF-1*, *Nos1*, and two positive controls (*COX2* and *COX6c*) were significantly reduced in both N2a cells and primary neurons transfected with shRNA as compared to those transfected with empty vectors. The extent of reduction ranged between 70 to 85% ($P < 0.01 – 0.001$). On the other hand, the expression of *Nos2*, *Nos3*, and nuclear respiratory factor 2α (another transcription factor) remained unchanged. The normal levels of *Nos2* and *Nos3* mRNA in both N2a cells and primary neurons were ~ 14 – 30% and 25 – 50%, respectively, as compared to that of *Nos1* (data not shown). The scrambled shRNA also did not have any effect on any mRNA level tested (Fig. 4B–C).

Response of *Nos1* gene promoter to KCl depolarizing stimulation

To determine if depolarizing stimulation altered the expression of *Nos1* gene in N2a cells, 20 mM of potassium chloride was added to the culture media for 5 hours, a mild regimen previously found to activate *NRF-1* and *COX* gene expression in primary neurons [21,33–34]. As shown in Figure 5A for N2a cells, depolarizing stimulation resulted in a significant increase (~120%) in the activity of *Nos1* promoter as monitored by luciferase assays ($P < 0.05 – 0.01$). This increase was abolished by mutating the NRF-1 site, confirming a link between KCl–induced depolarization and the activation of *Nos1* via NRF-1 binding.

Effect of NRF-1 silencing on KCl stimulation of *NOS1* and *COX* subunit gene expression

To determine if NRF-1 silencing affected the expression of *NOS* and *COX* subunit genes, N2a cells were transfected with NRF-1 shRNA for 48 hours and then subjected to 20 mM of KCl for 5 hours. As shown in Figure 5B, depolarizing stimulation resulted in a 185% to 198% increase in the expression of *Nos1*, *COX2*, and *COX6c* genes as monitored by real time quantitative PCR ($P < 0.05 – 0.01$) without affecting the expression of *Nos2* and *Nos3*. In the presence of NRF-1 silencing, however, KCl depolarization could no longer up-regulate the message levels of *Nos1, COX2*, and *COX6c*. These results confirmed the essential role of NRF-1 in the regulation of *Nos1 and COX* subunits in response to changing neuronal activity.

NRF-1 over-expression increased *Nos* and *COX* subunit mRNA levels and rescued neurons from tetrodotoxin-induced transcript reduction

A low concentration of TTX (0.4 μM) has been shown to decrease levels of *COX* subunit mRNAs as well as COX enzyme activity *in vivo* and in primary neurons [11,34].To determine if over-expression of NRF-1 could rescue not only *COX* but also *Nos1* transcript, a pSG5NRF-1 construct (gift of Dr. Richard Scarpulla) for NRF-1 over-expression was transfected into primary neurons that were then exposed to TTX (0.4 μM) for 3 days. When neurons were transfected with empty vectors, exposure to TTX led to a 52% reduction in *NRF-1* and a 71 – 75% reduction in *Nos1*, *Nos2*, *Nos3*, *COX2*, and *COX6C* mRNA levels (Figs. 6A–F), indicating an overall suppressive effect of TTX on gene expression in neurons. Neurons transfected with the pSG5NRF-1 construct had a 600% increase in mRNA levels of NRF-1 ($P < 0.001$) (Fig. 6A) and a 64 – 78% increase in those of *Nos1*, *COX2*, and *COX6C* ($P < 0.05 – 0.01$) as compared to empty vector controls (Figs. 6B–D). No change in *Nos2* and *Nos3* levels was evident (Fig. 6E – F). When exposed to TTX, neurons transfected with pSG5NRF-1 expressed 45 – 57% more *Nos1*, *COX2*, and *COX6C* transcripts as compared to those with empty vectors ($P < 0.05–0.01$) (Fig. 6A–D). No increase was found for *Nos2* and *Nos3* (Fig. 6E–F). The expression of NRF-1 itself was 286% higher in pSG5NRF-1-transfected neurons than those with empty vectors in the presence of TTX ($P < 0.001$) and 234% higher in the absence of TTX ($P < 0.001$). These results confirmed that NRF-1 could rescue *Nos1* and *COX* subunit mRNAs but not those of *Nos2* and *Nos3* in the presence of TTX.

Effect of NRF-1 silencing on guanylyl cyclase activity

To determine if NRF-1 also played an important role in regulating guanylyl cyclase, a downstream target of NO pathway, the promoter region of soluble guanylyl cyclase gene (*Gucy1a2*) was analyzed i*n silico*, and a potential NRF-1 binding was found. shRNA knockdown of NRF-1 resulted in an 80% decrease in the expression of *Gucy1a2* as compared to empty vector controls ($P < 0.01$) (Fig. 7). Scrambled shRNA had no effect. Future studies will determine if NRF-1 regulates *Gucy1a2* directly or indirectly.

DISCUSSION

The present study documents with multiple approaches that NRF-1 co-regulates *COX* and *Nos1*, but not *Nos2* and *Nos3* genes, thereby linking glutamatergic NOS-mediated synaptic transmission and energy metabolism at the transcriptional level of regulation in neurons. There is high homology in NRF-1 binding sites for *Nos1* (Table 1) and *COX* subunit promoters [13] among mice, rats, and humans, emphasizing the conservation of such co-regulation through evolution. With depolarizing neuronal activity, NRF-1 itself is activated at both protein and mRNA levels [21, the present study], and it, in turn, synchronizes the transcriptional activation of both *Nos1* and *COX* subunit genes, thereby ensuring that neuronal activity and energy metabolism remain tightly coupled.

NOS enzymes constitute a family of proteins with varying functions [35]. NOS1 is neuronal and is present at low concentrations in many cells but at high concentrations in a select group of neurons, primarily GABAergic ones [36–37]. NOS2 is typically not present in unstimulated cells, but is expressed in response to cytokines, lipopolysaccharides, and immunological challenges in macrophages [38–40]. NOS3 is expressed mainly in vascular endothelial cells and plays an important role in the regulation of vascular tone and tissue perfusion [39–41]. NRF-1 functionally binds to *Nos1* but not *Nos2* and *Nos3* promoters in neurons, and NRF-1 silencing down-regulates both protein and mRNA expression of COX and NOS1 without affecting NOS2 and NOS3 [the present study]. Thus, NRF-1's regulation of *Nos1* is linked to neuronal functioning and not to the production of NO *per se*. It also suggests that the transcriptional regulation of *Nos1* is very different from those of *Nos2* and *Nos3*. Each isoform,

in turn, mediates different cellular functions, including the regulation of various gene expression [35]. A fourth type of NOS is reportedly present in the mitochondria [42]. However, NO-dependent mitochondrial biogenesis in the murine subcortex is mediated by the NOS1 isoform [43]. Moreover, cardiomyocytes from neuronal NOS-knockout mice do not produce NO in the mitochondria, unlike those of the wild-type, confirming that the mitochondrial NOS (mtNOS) is actually a neuronal NOS [44]. MtNOS is reportedly involved in the regulation of oxidative phosphorylation, as NO can react with COX [42]. However, recent reports indicate that NO produced in the mitochondria by mtNOS (NOS1) in fact protects COX from external inhibitors [6,45]. The current study confirms the relation between COX and NOS1, and not with NOS2 and NOS3.

The level of COX activity in the normal monkey retina, monkey visual cortex, and cultured rat primary neurons are positively correlated with the density of distribution of excitatory neurotransmitters and their receptors, such as glutamate, NMDA receptor subunit NR1, and NOS1 [11–12,46–49]. This is consistent with the fact that repolarization after excitation-induced depolarization is highly energy-dependent and consumes the bulk of ATP produced in the CNS [8]. However, when neuronal activity is altered, such as afferent impulse blockade by TTX or depolarizing treatment with KCl, neuronal COX activity is adjusted to match the new energy demand [8,11]. NOS1 expression is also regulated by changes in neuronal activity [37,50]. At the transcriptional level, this regulation involves NRF-1 (present study). Thus, KCl-medited depolarization increases neuronal activity and up-regulates both *Nos1* and *COX* transcripts, but NRF-1 silencing with RNA interference prevented the up-regulation of *Nos1* and *COX* in the presence of KCl stimulation. The up-regulation of *Nos1* could be limited, as excess production of NO may induce glutamate toxicity [7]. On the other hand, TTX-mediated impulse blockade down-regulates both *Nos1* and *COX* transcripts, and over-expression of NRF-1 is able to rescue both *Nos1* and *COX* mRNAs from the suppressive effect of TTX. These results confirm the significant role of NRF-1 in regulating both *Nos1* and *COX* gene expression in neurons [13,the present study].

NRF-1, a phosphoprotein, is a transcriptional activator of nuclear genes encoding a number of mitochondrial respiratory enzymes, including subunits of the five respiratory chain complexes [51–52]. In fact, all ten nuclear-encoded subunit genes of complex IV (*COX*) are regulated by NRF-1 in neurons [13]. NRF-1 also activates the promoters of mitochondrial transcription factor A (*Tfam*), transcription specificity factors (*TFB1M* and *TFB2M*), and RNA-processing proteins required for mtDNA transcription and replication [16,19]. Thus, NRF-1 indirectly regulates the expression of the largest 3 COX subunit genes encoded in the mtDNA, and effectively regulates all 13 COX subunits. NRF-1 is vital for normal cell growth, cell function, and mitochondrial biogenesis [51–52], and its knockout is embryonically lethal [53]. Based on the present and our previous studies [13–14,26], the traditional consensus sequence for NRF-1 binding (YGCGCAYGCGCR) needs to be modified to include an invariant GCA core flanked by GC-rich sequences on either side, with the exact sequence of GC being variable, especially in rodents.

In response to glutamate, NOS1 is activated by the influx of calcium via NMDA receptors, and NO is produced to stimulate guanylyl cyclase to convert GTP to cGMP, an important second messenger that mediates neurotransmission [3–4,7]. The fact that NRF-1 regulates critical subunit genes of NMDA receptors [14], NOS1 (present study), and possibly guanylyl cyclase via either direct or indirect pathway (present study) strongly indicates that NRF-1 is intimately associated with the coordinated regulation of key neurochemicals associated with a major glutamatergic synaptic pathway in neurons (Fig. 8).

In conclusion, our findings confirm the tight coupling between neuronal activity and energy metabolism beyond the cellular level [8] to the molecular level. By having the *same*

transcription factor participate in the regulation of both processes, this tight coupling can be initiated and/or maintained at the transcriptional level. NRF-1 can effectively coordinate the expression of both *Nos1* and *COX* subunit genes, thereby coordinating a controlled and stable interplay between energy utilization of synaptic transmission and energy production. These findings beg many other questions. For example, do other transcription factors participate in the co-regulation of *Nos1* and *COX*? AP1, Sp1, CREB or NF-kB binding sites have been reported for *Nos1* promoters in humans and rats [17,54], but they have not been functionally characterized in neurons. Their roles in regulating energy metabolism, if present, have not been defined. Other likely candidates for co-regulation are nuclear respiratory factor 2 (NRF-2) and the coactivator peroxisome proliferator-activated receptor-γ coactivator 1α (PGC-1α). Previously, we have shown that NRF-2 also regulates all 13 *COX* subunits from the two genomes [18,20]. NRF-2 binding sites appear to be present on the murine *Nos1* promoter (our unpublished observations). PGC-1α is known to stimulate a powerful induction of both NRF-1 and NRF-2 [55] as well as binds to and co-activates NRF-1 in stimulating *Tfam* expression [20]. In primary neurons, PGC-1α responds to changing neuronal activity earlier than those of NRF-1 and NRF-2 [33,56]. Thus, for co-regulating neuronal activity and energy metabolism, the transcriptional mechanism is likely to engage many, if not all, of these key factors. Research is underway to explore these possibilities.

ACKNOWLEDGMENTS

It gives us great pleasure to thank Dr. Richard Scarpulla for his generous gift of NRF-1 antibodies and *pSG5NRF-1* plasmid and for his critical reading of the paper. We thank Dr. P. Aebischer for his gift of *pLVTHM* and Drs. S. Ongwijitwat and H. Meng for assisting in the construction of shRNA vectors. Supported by NIH Grant EY018441.

REFERENCES

1. Ignarro LJ. A novel signal transduction mechanism for transcellular communication. Hypertension 1990;5:477–483. [PubMed: 1977698]
2. Moncada S, Higgs A. The L-arginine-nitric oxide pathway. N. Engl. J. Med 1993;329:20002–20012.
3. Garthwaite J. Glutamate, nitric oxide and cell-cell signalling in the nervous system. Trends Neurosci 1991;14:60–67. [PubMed: 1708538]
4. Garthwaite J. Concepts of neural nitric oxide-mediated transmission. Eur.J.Neurosci 2008;11:2783–2802. [PubMed: 18588525]
5. Nathan C, Xie QW. Nitric oxide synthases: roles, tolls, and controls. Cell 1994;78:915–918. [PubMed: 7522969]
6. Garthwaite J, Boulton CL. Concepts of neural nitric oxide-mediated transmission. Annu. Rev. Physiol 1995;57:683–706. [PubMed: 7539993]
7. Dawson TM, Dawson VL. Nitric oxide synthase: Role as a transmitter/mediator in the brain and endocrine system. Ann. Rev. Med 1996;47:219–227. [PubMed: 8712777]
8. Wong-Riley MT. Cytochrome oxidase: an endogenous metabolic marker for neuronal activity. Trends Neurosci 1989;12:94–101. [PubMed: 2469224]
9. Wong-Riley, MTT. Primate visual cortex: dynamic metabolic organization and plasticity revealed by cytochrome oxidase. In: Peters, A.; Rockland, K., editors. Cerebral Cortex, Primary Visual Cortex in Primates. Vol. 10. New York: Plenum Press; 1994. p. 141-200.
10. Wikström, M.; Krab, K.; Saraste, M. A Synthesis. New York: Academic Press; 1981. Cytochrome Oxidase.
11. Wong-Riley MT, Huang Z, Liebl W, Nie F, Xu H, Zhang C. Neurochemical organization of the macaque retina: effect of TTX on levels and gene expression of cytochrome oxidase and nitric oxide synthase and on the immunoreactivity of Na+ K+ ATPase and NMDA receptor subunit I. Vision Res 1998;38:1455–1477. [PubMed: 9667011]
12. Zhang C, Wong-Riley MT. Do nitric oxide synthase, NMDA receptor subunit R1 and cytochrome oxidase co-localize in the rat central nervous system? Brain Res 1996;729:205–215. [PubMed: 8876989]

13. Dhar SS, Ongwijitwat S, Wong-Riley MT. Nuclear respiratory factor 1 regulates all ten nuclear-encoded subunits of cytochrome c oxidase in neurons. J. Biol. Chem 2008;283:3120–3129. [PubMed: 18077450]

14. Dhar SS, Wong-Riley MT. Coupling of energy metabolism and synaptic transmission at the transcriptional level: role of nuclear respiratory factor 1 in regulating both cytochrome c oxidase and NMDA glutamate receptor subunit genes. J. Neurosci 2009;29:483–492. [PubMed: 19144849]

15. Evans MJ, Scarpulla RC. NRF-1, a trans-activator of nuclear-encoded respiratory genes in animal cells. Genes Dev 1990;4:1023–1034. [PubMed: 2166701]

16. Scarpulla RC. Nuclear control of respiratory chain expression by nuclear respiratory factors and PGC-1-related coactivator. Ann. N. Y. Acad. Sci 2008;1147:321–334. [PubMed: 19076454]

17. Hall AV, Antoniou H, Wang Y, Cheung AH, Arbus AM, Olson SL, Lu WC, Kau CL, Marsden PA. Structural organization of the human neuronal nitric oxide synthase gene (NOS1). J. Biol. Chem 1994;52:33082–33090. [PubMed: 7528745]

18. Ongwijitwat S, Wong-Riley MT. Is nuclear respiratory factor 2 a master transcriptional coordinator for all ten nuclear-encoded cytochrome c oxidase subunits in neurons? Gene 2005;360:65–77. [PubMed: 16126350]

19. Gleyzer N, Vercauteren K, Scarpulla RC. Control of mitochondrial transcription specificity factors (TFB1M and TFB2M) by nuclear respiratory factors (NRF-1 and NRF-2) and PGC-1 family coactivators. Mol Cell Biol 2005;25:1354–1366. [PubMed: 15684387]

20. Ongwijitwat S, Liang HL, Graboyes EM, Wong-Riley MT. Nuclear respiratory factor 2 senses changing cellular energy demands and its silencing down-regulates cytochrome oxidase and other target gene mRNAs. Gene 2006;374:39–49. [PubMed: 16516409]

21. Yang SJ, Liang HL, Wong-Riley MT. Activity-dependent transcriptional regulation of nuclear respiratory factor-1 in cultured rat visual cortical neurons. Neuroscience 2006;141:1181–1192. [PubMed: 16753268]

22. Tomlinson DC, Hurst CD, Knowles MA. Knockdown by shRNA identifies S249C mutant FGFR3 as a potential therapeutic target in bladder cancer. Oncogene 2007;26:5889–5899. [PubMed: 17384684]

23. Sun D, Melegari M, Sridhar S, Rogler CE, Zhu L. Multi-miRNA hairpin method that improves gene knockdown efficiency and provides linked multi-gene knockdown. Biotechniques 2006;41:59–63. [PubMed: 16869514]

24. Livak KJ, Schmittgen TD. Analysis of relative gene expression data using realtime quantitative PCR and the 2(-delta delta C(T)). Methods 2001;25:402–408. [PubMed: 11846609]

25. Virbasius CA, Virbasius JV, Scarpulla RC. NRF-1, an activator involved in nuclear-mitochondrial interactions, utilizes a new DNA-binding domain conserved in a family of developmental regulators. Genes Dev 1993;7:2431–2445. [PubMed: 8253388]

26. Dhar SS, Liang HL, Wong-Riley MT. Nuclear respiratory factor 1 co-regulates AMPA glutamate receptor subunit 2 and cytochrome c oxidase: Tight coupling of glutamatergic transmission and energy metabolism in neurons. J Neurochem 2009;108:1595–1606. [PubMed: 19166514]

27. Boissel JP, Schwarz PM, Förstermann U. Neuronal-type NO synthase: transcript diversity and expressional regulation. Nitric Oxide 1998;5:337–349. [PubMed: 10100489]

28. Bros M, Boissel JP, Gödtel-Armbrust U, Förstermann U. Transcription of human neuronal nitric oxide synthase mRNAs derived from different first exons is partly controlled by exon 1-specific promoter sequences. Genomics 2006;4:463–473. [PubMed: 16413742]

29. Thierry-Mieg D, Thierry-Mieg J. AceView: a comprehensive cDNA-supported gene and transcripts annotation. Genome Biol 2006;7:1–4. [PubMed: 16925834]S12

30. Lang G, Gombert WM, Gould HJ. A transcriptional regulatory element in the coding sequence of the human Bcl-2 gene. Immunology 2005;114:25–36. [PubMed: 15606792]

31. Barthel KK, Liu X. A transcriptional enhancer from the coding region of ADAMTS5. PLoS ONE 2008;3:e2184. [PubMed: 18478108]

32. Tumpel S, Cambronero F, Sims C, Krumlauf R, Wiedemann LM. A regulatory module embedded in the coding region of Hoxa2 controls expression in rhombomere 2. Proc Natl Acad Sci U S A 2008;105:20077–20082. [PubMed: 19104046]

33. Liang HL, Wong-Riley MT. Activity-dependent regulation of nuclear respiratory factor-1, nuclear respiratory factor-2, and peroxisome proliferator-activated receptor gamma coactivator-1 in neurons. Neuroreport 2006;17:401–405. [PubMed: 16514366]
34. Liang HL, Ongwijitwat S, Wong-Riley MT. Bigenomic functional regulation of all 13 cytochrome c oxidase subunit transcripts in rat neurons in vitro and in vivo. Neuroscience 2006;140:177–190. [PubMed: 16542778]
35. Bogdan C. Nitric oxide and the regulation of gene expression. Trends Cell Biol 2001;11:66–75. [PubMed: 11166214]
36. Seress L, Abrahám H, Hajnal A, Lin H, Totterdell S. NOS-positive local circuit neurons are exclusively axo-dendritic cells both in the neo- and archicortex of the rat brain. Brain Res 2005;1056:183–190. [PubMed: 16102735]
37. Wong-Riley, MTT.; Nie, F.; Hevner, RF.; Liu, S. Brain cytochrome oxidase: functional significance and bigenomic regulation in the CNS. In: Gonzalez-Lima, F., editor. Cytochrome oxidase in Neuronal Metabolism and Alzheimer's Disease. New York: Plenum Press; 1998. p. 1-53.
38. de Vera ME, Shapiro RA, Nussler AK, Mudgett JS, Simmons RL, Morris SM, Billiar TR, Geller DA. Transcriptional regulation of human inducible nitric oxide synthase (NOS2) gene by cytokines: Initial analysis of the human NOS2 promoter. Proc. Natl. Acad. Sci. USA 1996;93:1054–1059. [PubMed: 8577713]
39. Kröncke KD, Fehsel K, Kolb-Bachofen V. Inducible nitric oxide synthase in human diseases. Clin. Exp. Immunol 1998;113:147–156. [PubMed: 9717962]
40. Mungrue IN, Bredt DS, Stewart DJ, Husain M. From molecules to mammals: what's NOS got to do with it? Acta Physiol. Scand 2003;179:123–135. [PubMed: 14510775]
41. Li H, Wallerath T, Forstermann U. Physiological mechanisms regulating the expression of endothelial-type NO synthase. Nitric Oxide 2002;7:132–147. [PubMed: 12223183]
42. Bates TE, Loesch A, Burnstock G, Clark JB. Mitochondrial nitric oxide synthase: a ubiquitous regulator of oxidative phosphorylation? Biochem Biophys Res Commun 1996;218:40–44. [PubMed: 8573169]
43. Gutsaeva DR, Carraway MS, Suliman HB, Demchenko IT, Shitara H, Yonekawa H, Piantadosi CA. Transient hypoxia stimulates mitochondrial biogenesis in brain subcortex by a neuronal nitric oxide synthase-dependent mechanism. J. Neurosci 2008;28:2015–2024. [PubMed: 18305236]
44. Kanai AJ, Pearce LL, Clemens PR, Birder LA, VanBibber MM, Choi SY, de Groat WC, Peterson J. Identification of a neuronal nitric oxide synthase in isolated cardiac mitochondria using electrochemical detection. Proc. Natl. Acad. Sci. U S A 2001;98:14126–14131. [PubMed: 11717466]
45. Collman JP, Dey A, Decreau RA, Yang Y, Hosseini A, Solomon EI, Eberspacher TA. Interaction of nitric oxide with a functional model of cytochrome c oxidase. Proc. Natl. Acad. Sci. U S A 2008;105:9892–9896. [PubMed: 18632561]
46. Nie F, Wong-Riley MT. Mitochondrial-, nuclear-encoded subunits of cytochrome oxidase in neurons: differences in compartmental distribution, correlation with enzyme activity, and regulation by neuronal activity. J Comp. Neurol 1996;373:139–155. [PubMed: 8876469]
47. Wong-Riley MTT, Jacobs P. AMPA glutamate receptor subunit 2 in normal and visually deprived macaque visual cortex. Vis. Neurosci 2002;19:563–573. [PubMed: 12507323]
48. Zhang C, Wong-Riley M. Expression and regulation of NMDA receptor subunit R1 and neuronal nitric oxide synthase in cortical neuronal cultures: correlation with cytochrome oxidase. J Neurocytol 1999;28:525–539. [PubMed: 10800203]
49. Zhang C, Wong-Riley MT. Depolarizing stimulation upregulates GA-binding protein in neurons: a transcription factor involved in the bigenomic expression of cytochrome oxidase subunits. Eur. J. Neurosci 2000;12:1013–1023. [PubMed: 10762332]
50. Tascedda F, Molteni R, Racagni G, Riva MA. Acute and chronic changes in K+-induced depolarization alter NMDA and nNOS gene expression in cultured cerebellar granule cells. Mol. Brain Res 1996;40:171–174. [PubMed: 8840029]
51. Scarpulla RC. Nuclear control of respiratory gene expression in mammalian cells. J Cell Biochem 2006;97:673–683. [PubMed: 16329141]
52. Scarpulla RC. Transcriptional paradigms in mammalian mitochondrial biogenesis and function. Physiol. Rev 2008;88:611–638. [PubMed: 18391175]

53. Huo L, Scarpulla RC. Mitochondrial DNA instability and peri-implantation lethality associated with targeted disruption of nuclear respiratory factor 1 in mice. Mol Cell Biol 2001;21:644–654. [PubMed: 11134350]

54. Sasaki M, Gonzalez-Zulueta M, Huang H, Herring WJ, Ahn S, Ginty DD, Dawson VL, Dawson TM. Dynamic regulation of neuronal NO synthase transcription by calcium influx through a CREB family transcription factor-dependent mechanism. Proc. Natl. Acad. Sci. U S A 2000;97:8617–8622. [PubMed: 10900019]

55. Wu Z, Puigserver P, Andersson U, Zhang C, Adelmant G, Mootha V, Troy A, Cinti S, Lowell B, Scarpulla RC, Spiegelman BM. Mechanisms controlling mitochondrial biogenesis and respiration through the thermogenic coactivator PGC-1. Cell 1999;98:115–124. [PubMed: 10412986]

56. Meng H, Liang HL, Wong-Riley M. Quantitative immuno-electron microscopic analysis of depolarization-induced expression of PGC-1alpha in cultured rat visual cortical neurons. Brain Res 2007;1175:10–16. [PubMed: 17870059]

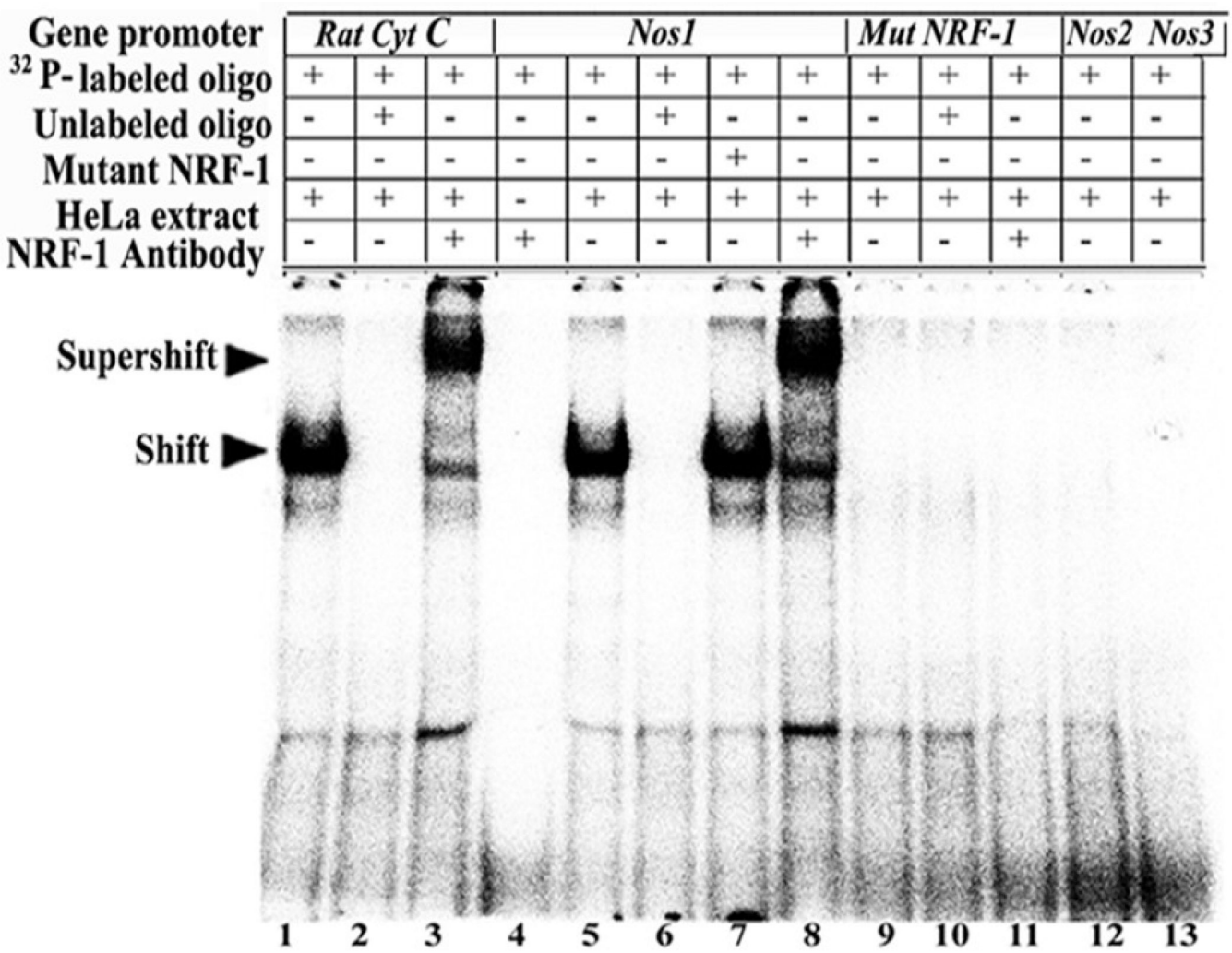

Fig. 1. NRF-1 interactions in-vitro and in-vivo with NOS isoform genes and promoter mutational analysis

EMSAs for NRF-1. ^{32}P- labeled oligonucleotides, excess unlabeled oligos as competitors, excess unlabeled mutant NRF-1 as competitors, HeLa extract, and NRF-1 antibodies are indicated by a + or a − sign. Arrowheads indicate NRF-1 shift and supershift complexes. The positive control, *cytochrome c*, shows a shift (A, lane 1) and a supershift (A, lane 3) band. When excess unlabeled competitor was added, it did not yield any band (A, lane 2). *Nos1* subunit showed specific shift and supershift bands that were eliminated by excess unlabeled competitors (A, lanes 5, 8 & 6, respectively), while *Nos2* and *Nos3* showed no shift bands (A, lanes 12–13). Labeled mutated NRF-1 site on *Nos1* was used as a negative control, and it did not yield any band (A, lanes 9–11). Excess unlabeled but mutated NRF-1 site could not compete (A, lane 7). Labeled oligos with NRF-1 antibodies alone with no HeLa extract did not yield any band (A, lane 4).

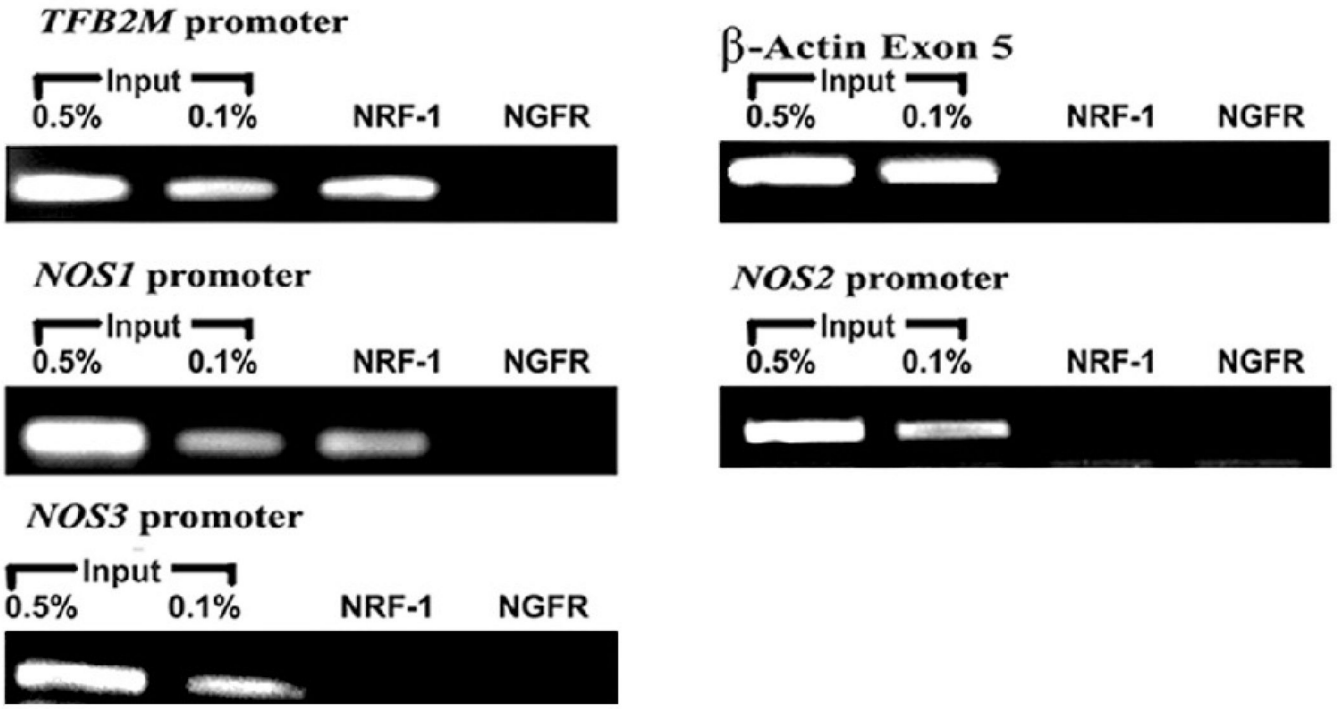

Fig. 2. ChIP assays

Input lanes represent 0.5% and 0.1% of chromatin. *TFB2M* promoter was the positive control and β-actin was the negative control. *Nos1* promoter immunoprecipitated with NRF-1, while *Nos2* and *Nos3* did not. Anti-nerve growth factor receptor p75 antibodies (NGFR) represent a negative control.

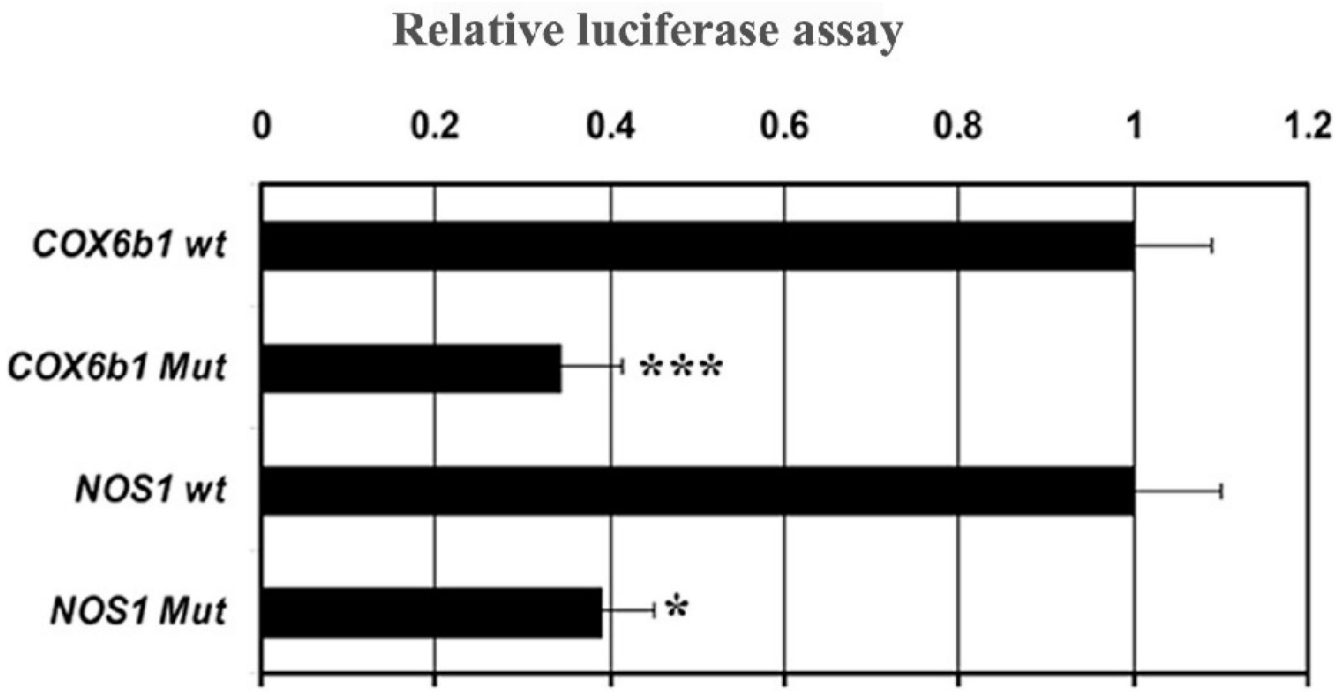

Fig. 3. Site-directed mutations of NRF-1 binding sites on *Nos1* and *COX6b1* promoters

Mutated NRF-1 binding sites on *Nos1 and COX6b1* subunit resulted in significant reductions in luciferase activity as compared to wild type (wt). (N = 6 for each construct). *, $P < 0.05$, ***, $P < 0.001$.

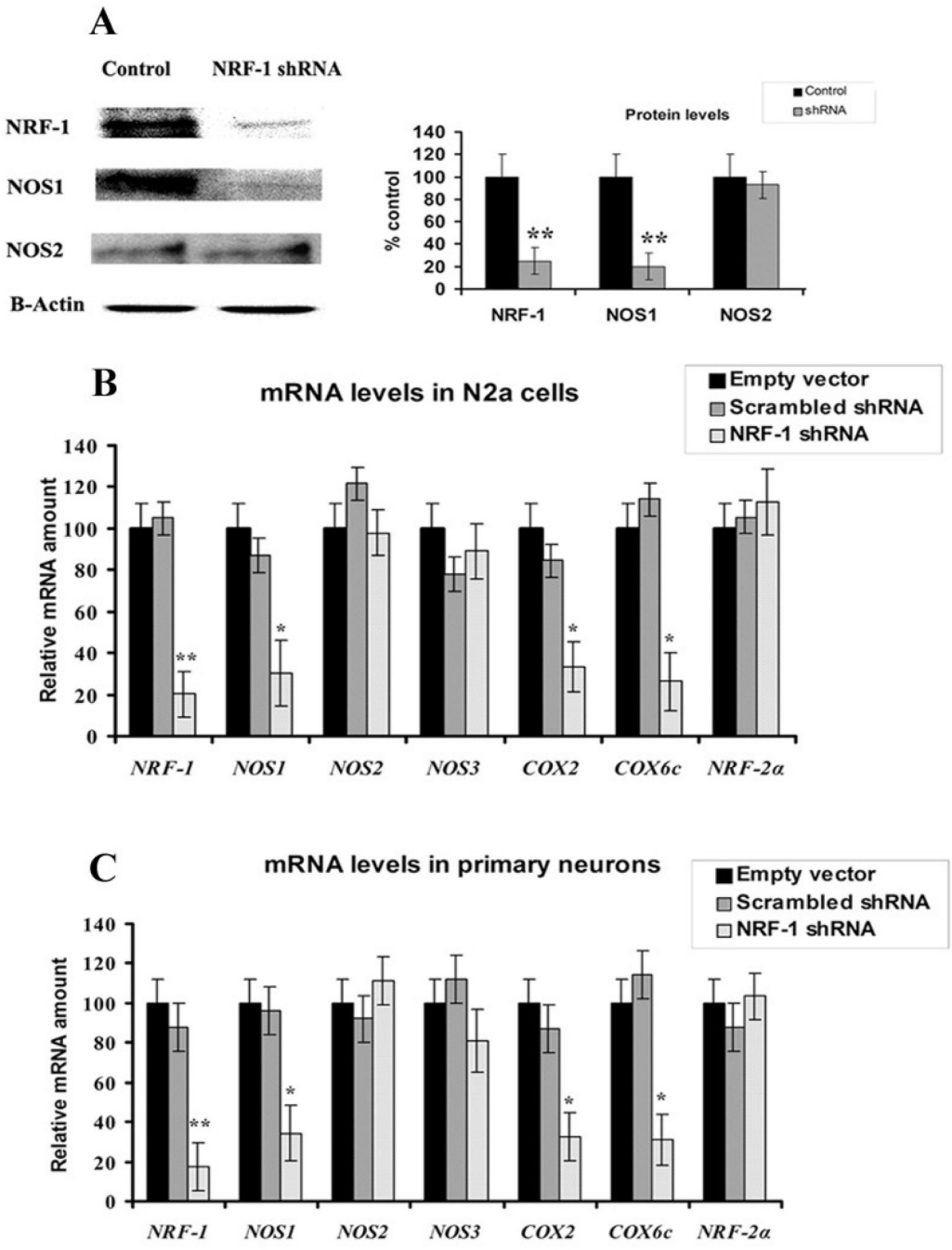

Fig. 4. NRF-1 silencing suppresses *Nos1* and *COX* subunit mRNAs

(A) Western blot reveals a down-regulation of NRF-1 and NOS1 protein levels in NRF-1 shRNA-transfected neuron, whereas NOS2 protein levels were not affected. β-Actin served as a loading control. (B–C) N2a cells and primary neurons were transfected with shRNA against NRF-1 (*light gray bars*), or with empty vectors (*black bars*), or with scrambled shRNA (*dark gray bars*). NRF-2α served as a negative control. *NRF-1*, *Nos1*, *COX2*, and *COX6c* subunit mRNAs show significant decreases in shRNA-treated samples as compared to those with empty vectors, whereas *Nos2*, *Nos3*, and *NRF-2α* mRNA remained unchanged. N = 6 for each data point. *, $P < 0.05$; **, $P < 0.01$ as compared to empty vectors.

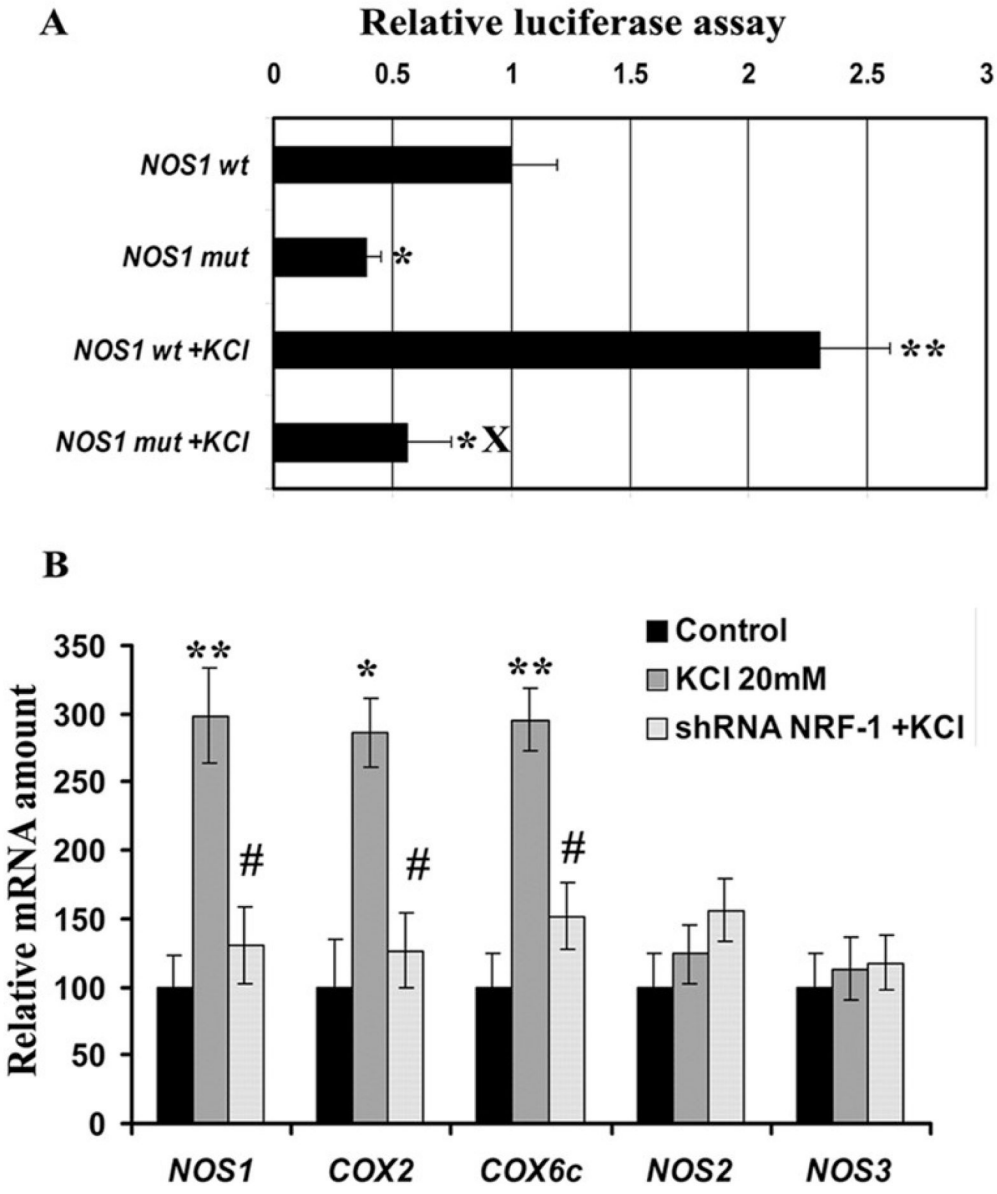

Fig. 5. Depolarization-induced up-regulation of promoter gene expression and mRNA levels of NOS and COX subunits in neurons

(A) Site-directed mutations of NRF-1 binding sites on *Nos1* promoter resulted in a significant reduction in luciferase activity as compared to the wild type (wt). KCl depolarization increased promoter activity in the wild type but not in the mutated *Nos1*. (N = 6 for each construct). *, $P < 0.05$, **, $P < 0.01$ as compared to *Nos1* wild type. X = $P < 0.01$ as compared to *Nos1* wt with KCl depolarization. (B) Data from real time quantitative PCR indicate that *Nos1*, *COX2*, and *COX6c* gene expression in N2a cells were increased by KCl depolarization as compared to controls, whereas those of *Nos2* and *Nos3* were not affected by KCl. NRF-1 silencing with shRNA prevented the up-regulation of *Nos1*, *COX2*, and *COX6c* mRNAs by KCl. Again, *Nos2* and *Nos3* were not affected. Values represent mean ± S.E.M of combined data from 3 independent experiments. * $P < 0.05$, ** $P < 0.01$ versus controls. All $^{\#}P$ values were compared to 20 mM KCl-treated samples ($^{\#}P < 0.05$). *Nos2* and *Nos3* levels were not significantly different from controls.

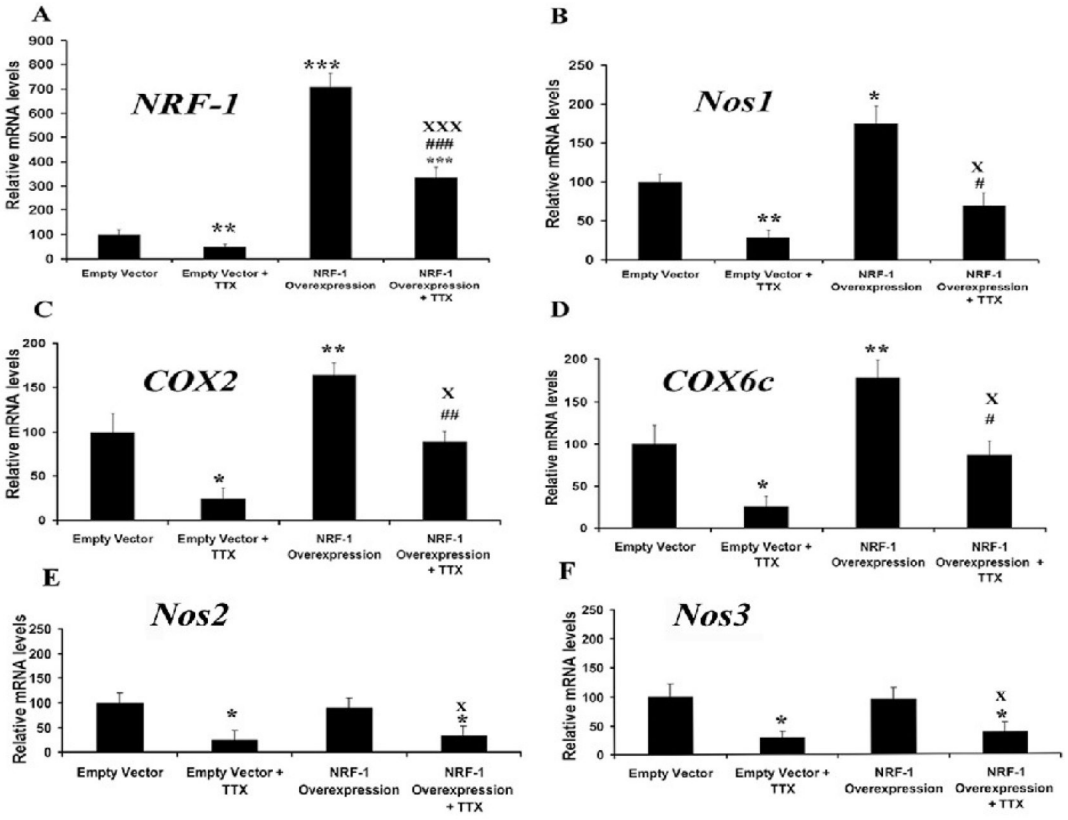

Fig. 6. NRF-1 over-expression in primary neurons significantly increased mRNA levels for *Nos1*, *COX2*, and *COX6c* genes and rescued them from TTX-induced suppression

NRF-1, *Nos1*, *COX2*, *COX6c*, *Nos2*, and *Nos3* mRNA levels (A–F) were all reduced by TTX as compared to controls. Over-expression of NRF-1 significantly increased transcript levels of *NRF-1*, *Nos1*, *COX2*, and *COX6c*, but not of *Nos2* and *Nos3*. Over-expression of NRF-1 was able to rescue *NRF-1*, *Nos1*, *COX2*, and *COX6c*, but not *Nos2* and *Nos3*. Group means were analyzed for overall statistical significance using the Student's *t*-test (N = 6 for each group). All * *P* values were compared to empty vectors (* $P < 0.05$, ** $P < 0.01$, *** $P < 0.001$). All $^{\#}$ *P* values were compared to empty vector + TTX ($^{\#}P < 0.05$, $^{\#\#}P < 0.01$, $^{\#\#\#}P < 0.001$), and all ^{X} *P* values were compared to NRF-1 over-expression ($^{X}P < 0.05$, $^{XXX}P < 0.001$).

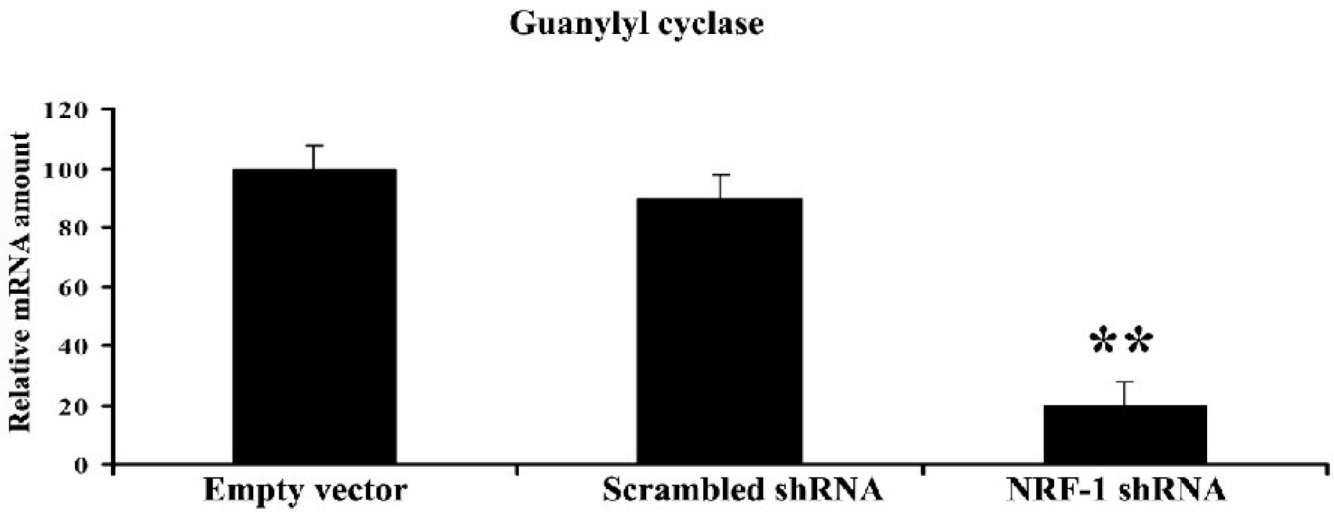

Fig. 7. NRF-1 silencing suppresses mRNA level in guanylyl cyclase gene

N2a cells were transfected with shRNA against NRF-1, or with empty vector, or with scrambled shRNA. Guanylyl cyclase (*Gucy1a2*) mRNA shows significant decrease in shRNA-treated samples as compared to those with empty vectors. N = 6 for each data point. *, $P < 0.01$. Scrambled shRNA did not cause any change in *Gucy1a2 levels.*

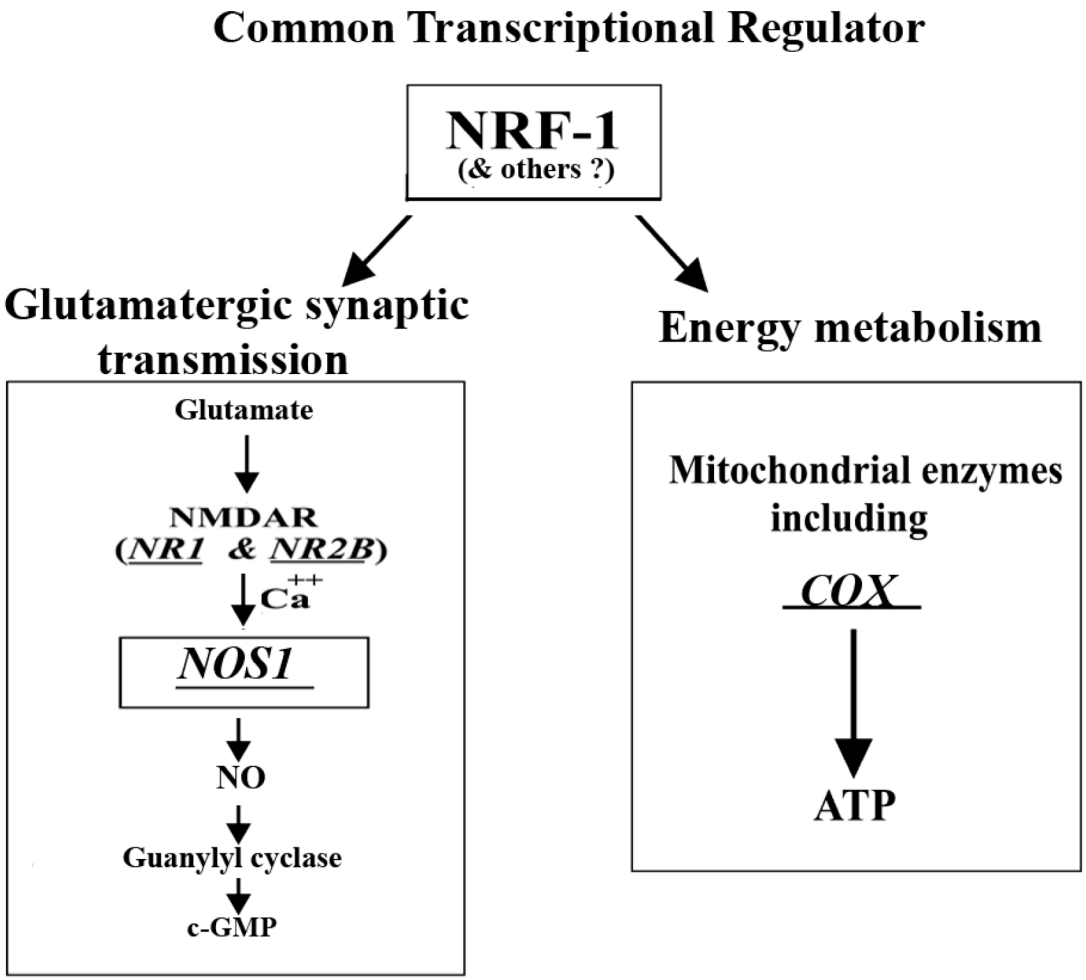

Fig. 8. Schematic representation of *Nos1* regulation via NRF-1

A working model indicating that energy metabolism and neuronal activity are tightly coupled. NMDAR (*NR1* and *NR2B*) (Dhar and Wong-Riley, 2009), *COX* subunits (Dhar et al., 2008) and *Nos1* (present study) are all co-regulated by the same transcription factor, NRF-1. A downstream mediator of NOS1 pathway, guanylyl cyclase, also has a potential NRF-1 binding site. Thus, NRF-1 is intimately associated with the coordinated regulation of energy metabolism as well as key neurochemicals associated with a major glutamatergic synaptic pathway in neurons.

Table 1

Aligned partial sequences of *Nos1* promoters from rat (R), mouse (M), and human (H) genomes show conservation of NRF-1 binding sites (in boldface)

Invariant GCA core sequences are underlined. Solid boxes highlight NRF-1 sites that are highly conserved in all three or at least two species.

NOS1

R		CGAGGAGGTGCT**GCGGAGCAGAGCGGC**CTT
M	+142	CGAGGAGGTGCC**GCGGAGCAGAGCGGC**CTT +171
H		CGTGGGGGCGCC**GCAGAGCAGAGTGGC**CTC

Table 2

Table 2A EMSA Probes

Positions of probes are given relative to TSP. Putative NRF-1 binding sites are in boldface. Mutated nucleotide sequences are underlined.

Gene Promoter	Position	Sequence
Nos1	+150/+164	F 5′TTTTGT**GCCGCGGAGCAGAGCGGC**CTT 3′ R 3′ CACGG**CGCCTCGTCTCGCCG**GAATTTT 5′
Nos2	−98/−73	F 5′TTTTAGTTATGCAAAATAGCTCTGCAGAG 3′ R 3′ TCAATACGTTTTATCGAGACGTCTCTTTT 5′
Nos3	−114/−89	F 5′TTTTCCACATTAAATACGCAACAAATAGA 3′ R 3′ GGTGTAATTTATGCGTTGTTTATCTTTTT 5′
Nos1 with mutated NRF-1 site	−49/−24	F 5′TTTTGT**AAA**GCGGA**AAA**GAGCGGCCTT 3′ R 3′ CA**TTT**CGCCT**TTT**CTCGCCGGAATTTT 5′
Rat *Cyt C*	−172/−147	F 5′TTTTCTGCTA**GCCCGCATGCGC**GCGCACCTTA3′ R 3′ GACGAT**CGGGCGTACGCG**CGCGTGGAATTTTT5′

Table 2B Chip Primers

Positions of amplicons are given relative to TSP.

Gene Promoter	Position	Sequence	Amplicon length
Nos1	−134 to +68	F 5′AAACGCAAAGTGGGAGGTCT 3′ R 5′GCATGGCTGGTTTACGTTTT 3′	202 bps
Nos2	−140 to +5	F 5′AGCTAACTTGCACACCCAACT 3′ R 5′GGGCCAGAGTCTCAGTCTTC 3′	145 bps
Nos3	−171 to +17	F 5′GGTATTTGATGCTCGGGACT 3′ R 5′CACTGTGATGGCTGAACTGA 3′	188 bps
TFB2M promoter	−64 to +115	F 5'GAAGCGAGTGAGCAAAGGAC 3' R 5'GGTCCCCTCATCCTCCTCTA 3'	179 bps
β-Actin exon 5	−134 to +53	F 5'GCTCTTTTCCAGCCTTCCTT 3' R 5'CGGATGTCAACGTCACACTT 3'	187 bps

Table 2C PCR cloning primers

NRF-1 mutated nucleotide sequences are in boldface.

Cloning Primers	Primer sequence
Nos1	F 5′AAGGTACCGCCAGGTGACCACCACTAAC 3′ R 5′AAAAGCTTCTGACGCATGGCTGGTTTAC 3′
MCOX6b1	F 5'AAGGTACCGCCAGCCCTTAATTGTTTTC3' R 5'AAAAGCTTTCGCAACTAAAAGCTCCACA 3'
Mutagenesis Primers	
Nos1Mut	F 5′ GAGGTGCCGCGGA**TTT**GAGCG**TT**CTTATCCAAGCC 3′ R 5′ GGCTTGGATAAG**AA**CGCTC**AAA**TCCGCGGCACCTC 3′
MCOX6b1Mut	F 5'CAGCACTAGTTAGGCAGAG**TTT**GGCGGATTTCTGAGTCTAC3' R 5'GTAGACTCAGAAATCCGCC**AAA**CTCTGCCTAACTAGTGCTGG 3'

Table 3

Primers for real-time PCR

Gene	Sequence	Amplicon length	T_m
Nos1	F 5′CTGGAGGAAGTAGCCAAGAAG 3′ R 5′TTCTCCATGGTTTGATGAAGG 3′	154	60°
Nos2	F 5′TGATCTTGTGCTGGAGGTGACCAT 3′ R 5′TGTAGCGCTGTGTGTCACAGAAGT 3′	200	60°
Nos3	F 5′TATTTGATGCTCGGGACTGCAGGA 3′ R 5′ACGAAGATTGCCTCGGTTTGTTGC 3′	92	60°
NRF-1	F 5′GGCACAGGCTGAGCTGATG 3′ R 5′CTAGTTCCAGGTCAGCCACCTTT 3′	90	59.5°
NRF-2α	F 5'CTCCCGCTACACCGACTAC 3' R 5'TCTGACCATTGTTTCCTGTTCTG 3'	145	59.5°
COX2	F 5′TGGCTTACAAGACGCTACATC 3′ R 5′GGAGGGAAGGGCAATTAGAA 3′	201	59.5°
COX6c	F 5'AGCGTCTGCGGGTTCATA 3' R 5'GCCTGCCTCATCTCTTCAAA 3'	154	60°
Gucy1a2	F 5′GTGCATATCCAGCAATGTTGAACGG 3′ R 5′CGTTGCAAACGGTGAATTATCCTGCC 3′	89	60°
β-Actin	F 5'GGCTGTATTCCCTCCATCG 3' R 5'CCAGTTGGTAACAATGCCATGT 3'	154	59.5
18S	F 5′CGCGGTTCTATTTTGTTGGT 3′ R 5′AGTCGGCATCGTTTATGGTC 3′	219	59.5°